Electrochemical Preparation of Conducting Polymer Microelectrodes

Maciej Mazur* and Pawel Krysinski

Laboratory of Electrochemistry, Department of Chemistry, University of Warsaw, 02-093 Warsaw, Pasteura 1, Poland

Received: May 7, 2002; In Final Form: August 1, 2002

The paper presents our results of studies on the synthesis of conducting polymer microislands using self-assembled thiol monolayers containing pinhole defects. It was found that in consequence of electrochemical oxidation of the corresponding monomers (aniline o-methoxyaniline 2,5-dimethoxyaniline) on gold coated with long-chain alkanethiols the polymer is being formed in a localized manner starting the growth from thiol film defects. Therefore, the conducting polymer microislands can be created on the thiol-coated substrate in such a way. The sizes and distribution of the synthesized microislands were estimated on the basis of microscopic and electrochemical measurements. It was found that the polymer microstructures can be switched between a conducting and nonconducting state by application of the appropriate potential to the metal electrode. When oxidized (conducting), the microstructures behave like an array of microelectrodes, but when reduced (nonconducting form), the whole thiol/polymer layer reveals blocking properties.

Introduction

The production of materials with micrometer- or submicrometer-scale patterns is of importance in a range of applications such as photonic materials,[1,2] high-density magnetic data storage devices,[3] microchip reactors,[4] and biosensors.[5] The candidates of choice can be conducting polymers with π-conjugated backbones which display unusual electronic properties such as low-energy optical transitions, low ionization potentials, and high electron affinities. This class of polymers can be oxidized or reduced more readily and more reversibly than conventional polymers.[6] Their interesting properties as well as their environmental stability in their conductive (doped) form makes them suitable to use in secondary batteries sensors, catalysts, electrochromic materials, and organic semiconductors.[6−9]

Although these materials are attractive from the standpoint of their electronic and physical properties, one significant limitation that remains is the ability of these materials to be processed into specific structures on an industrial scale. One means to accomplish the requisite level of processability is through the synthesis of conducting polymers in the presence of templates or molecular matrixes of predetermined structure. The use of templates allows substantial control upon the physical properties and topological structure of polymers, e.g., the formation of polymer mono- or multilayers, polymer brushes, polymer nanotubes, or nanoparticles.[10−20]

The aim of this work is to prepare polymer island structures distributed on a surface. The synthesis is based on preparation of a thin electrically insulating film on the metal (electrode) surface containing a number of "gate sites" and subsequent electrochemical deposition of the polymer selectively at these sites. The electrochemical polymer deposition reactions are strongly inhibited on film-coated regions of the surface and promoted at the gate sites.

The best candidates for electrode-bound thin insulating films are alkanethiol monolayers on gold. Because of their spontaneous strong adsorption onto gold alkanethiols can be used to prepare stable monomolecular films.[21−24] The formation of the gate sites within the film can be performed by two methods. The first method exploits the existence of defects (pinholes) within the monomolecular films. The defect sites (small areas of exposed metal surface) can act as nucleation sites for an electrochemical polymerization reaction allowing the deposition of polymeric materials.[19,20,25] The second method involves the formation of mixed alkanethiol monolayers containing molecules of different hydrocarbon chain length. As the deposition rate decreases exponentially with increasing film thickness, electrochemical deposition of the polymer will occur preferentially on regions modified with shorter thiol and will be attenuated on regions modified with longer.[26,27]

A key issue in this paper is the investigation of electrochemical properties of polymer structures deposited on a thiol-coated electrode. The fundamental feature of conducting polymers is their ability to switch between conducting (oxidized) and nonconducting (reduced) forms. As the majority of the metal surface is covered with a passivating thiol monolayer, the polymer microislands when oxidized by polarization of metal electrode to an appropriate potential can behave as an array of microelectrodes. When the polymer is reduced, the microislands are nonconductive and the thiol/polymer layer will behave as an insulator.

Experimental Section

Chemicals. All chemicals were commercially available and were used without purification: aniline (Fluka ≫99.5%), o-methoxyaniline (Aldrich 99+%), 2,5-dimethoxyaniline (Fluka 97%), tetradecanethiol−C_{14}SH (Fluka >98%), hexadecanethiol−C_{16}SH (Fluka ∼95%), octadecanethiol−C_{18}SH (Aldrich 98%), potassium hexacyanoferrate (II) $K_4Fe(CN)_6$ (POCh reagent grade), hexaaminеruthenium (III) chloride (Aldrich 98%), sulfuric acid H_2SO_4 (POCh 98%), potassium chloride KCl (POCh reagent grade), and methanol (POCh reagent grade). Deionized water was obtained through the Milli-Q system.

* To whom correspondence should be addressed. E-mail: mmazur@chem.uw.edu.pl.

10.1021/jp026077m CCC: $22.00
Published on Web 09/11/2002

Instrumentation and Procedures. Electrochemical measurements were conducted with PC-controlled custom-built potentiostat/galvanostat (KSP Electronics Poland) using a conventional small volume three-electrode cell with Pt wire as a counter electrode. All potentials are quoted vs Ag/AgCl/1M KCl_{aq} reference electrode. Polycrystalline gold electrodes (99.99% Au ball electrode 0.2 cm^2) were flamed in the reductive zone until almost melted then placed in deaerated 0.5 M H_2SO_4 aqueous solution. Cyclic voltammetry was used (scan range −300 + 1500 mV scan rate 100 mV/s) for electrochemical annealing of the electrode surface. Potential scans were repeated until the steady-state voltammograms were achieved.

Commercially available Nanoscope IIIa from Digital Instruments was used to collect the STM images presented in this paper. The microscope was run in the constant current mode. Tungsten tips were prepared by electrochemical etching of a 0.25 mm diameter wire in 4 M aqueous KOH as described elsewhere.[28]

Substrates used for STM measurements were microscope glass slides with evaporated 2 nm layer of chromium and 200 nm of gold (prepared in the Laboratory of Electrochemistry University of Florence Italy).

Solutions of hexaammineruthenium(III) chloride used for integrity studies of polymer layers were deaerated by bubbling with argon for 10 min before measurements.

Monolayers of corresponding thiols were assembled by immersing a gold electrode for at least 12 h into methanol solution containing 0.5 mM of the thiol. Afterward, the modified electrodes were rinsed with abundance of methanol followed by Milli-Q water and dried.

The polymers were deposited potentiostatically on electrodes from 50 mM of the corresponding monomer in aqueous 1 M H_2SO_4. After polymerization, the electrodes were rinsed with deionized water and dried.

Results and Discussion

Deposition of Conducting Polymers on Thiol-Modified Gold Electrodes. Three types of polymers—polyaniline (PANI), poly(o-methoxyaniline) (POMA), and poly(2,5-dimethoxyaniline) (PDMA)—were potentiostatically deposited on electrodes coated with monomolecular layers of alkanethiols containing hydrocarbon chains of different length: octadecanethiol ($C_{18}SH$), hexadecanethiol ($C_{16}SH$), and tetradecanethiol ($C_{14}SH$). As aniline o-methoxyniline and 2,5-dimethoxyaniline reveal different potentials of monomer oxidation, in order to provide comparable electropolymerization conditions, the PANI was prepared at the potential of 1000 mV POMA − 825 mV PDMA − 700 mV (monomer oxidation voltammetric peak potential plus 95 mV).

Figure 1 presents the curves of polymer potentiostatic deposition of respectively PANI, POMA, and PDMA on C_{18}-SH-coated gold. For these three cases, after the initial relatively large current flow associated mainly with the double layer charging, a decrease of current can be observed toward much smaller although nonzero values. This current can be assigned to oxidation of the monomers present in the solution and formation of the polymer. In all the cases, the curves observed are qualitatively similar although some differences in the magnitude of current are noticeable. It is difficult to unequivocally assign these differences to specified processes occurring during the polymerization. Our intention was to prepare polymers at comparable conditions although exactly identical current transients could not be obtained. We have noticed however that the results obtained for these three polymers when analyzed as a function of charge consumed for polymerization are substantially the same.

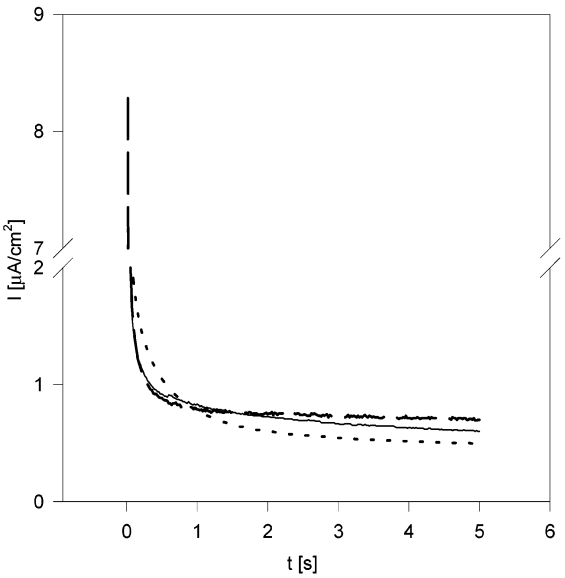

Figure 1. Comparison of potentiostatic deposition of PANI (solid line), POMA (dotted line), and PDMA (dashed line) on $C_{18}SH$-coated gold.

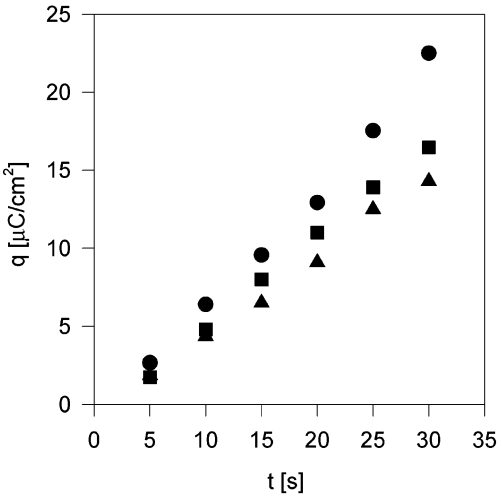

Figure 2. Dependence of polymerization charge of aniline with time: $C_{18}SH$ (circles), $C_{16}SH$ (squares), and $C_{14}SH$ (triangles).

The deposition curves for the electrodes covered with monolayers with hydrocarbon chains of different lengths are qualitatively identical. The only difference is the magnitude of current observed during polymerization of monomers. Figure 2 shows variation of the aniline electropolymerization charge on $C_{18}SH$ $C_{16}SH$ $C_{14}SH$ coated gold as a function of polymerization time.

From the presented dependencies, one can see that although the differences are rather small the oxidation rate of monomer decreases in the order $C_{18} > C_{16} > C_{14}$. This means that the rate of the polymerization increases with the increase of the thickness of the thiol monolayer. However, assuming the model that the electrons are tunneled through the monolayer, one should expect that the rate of the monomer oxidation decrease with the increase of film thickness according to the formula[29]

$$k = k^0 \exp(-\beta d)$$

This discrepancy between the experimental results and the

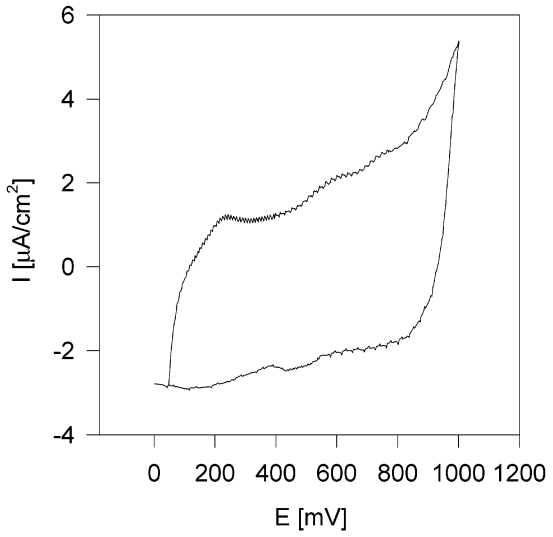

Figure 3. Cyclic voltammogram of PANI/C_{18}SH/gold electrode in aqueous 1 M H_2SO_4. Sweep speed 50 mV/s.

formula suggests that the deposition of the polymer must occur according to a different mechanism which will be discussed further.

Investigation of the Electrochemical Properties of the Thiol/Polymer Structure in the Supporting Electrolyte Solution. The thiol/polymer layers were voltammetrically studied in aqueous 1 M H_2SO_4 in the absence of the monomer in the solution. Figure 3 presents cyclic voltammogram recorded on the C_{18}SH-coated gold modified with PANI.

The curve reveals no characteristic signals attributable to PANI (the curve is similar also to voltammograms obtained for POMA and PDMA, not shown) and is characterized by low current magnitude. These two facts most probably derive from the very low amount of deposited polymer on the surface.

Investigation of Thiol/Polymer Layer in the Presence of Redox Probes. The electrochemical properties of thiol/polymer system were studied by cyclic voltammetry in the presence of $Fe(CN)_6^{4-}$ in the solution.

Prior to these studies we had checked the stability of the redox probe used, $Fe(CN)_6^{4-}$, in strongly acidic media 1 M H_2SO_4. We recorded voltammetric curve on bare gold (Figure 2 inset) and obtained a typical CV response for diffusion-controlled redox reaction which was stable during cycling. As our measurements of the thiol/polymer systems involved the recording of only one or two voltammetric curves per sample, there was practically no possibility of decomposition of the redox complex or formation of side products, e.g., prussian blue.[30] We should also stress that before each measurement a new solution of $Fe(CN)_6^{4-}$ was prepared.

In the potential range of ferrocyanide electroactivity, the studied polymers are in their oxidized conducting forms. It is feasible therefore to investigate how the deposited polymer affects the electrode reaction of $Fe(CN)_6^{4-}$ and on this basis to conclude on the properties and topological structure of the deposit. Figure 4 shows voltammetric curves of $Fe(CN)_6^{4-}$ oxidation on C_{18}SH and C_{18}SH/PANI-modified gold. The CV curve recorded for C_{18}SH-coated gold reveals low magnitude of current and approximately exponential shape (one can see a very small bend of the curve which may suggest the presence of a small amount of pinhole defects present in the monolayer acting as individual microelectrodes). The characteristics of the voltammogram confirm that the thiol monolayer nearly completely isolates the electrode metal from the solution.

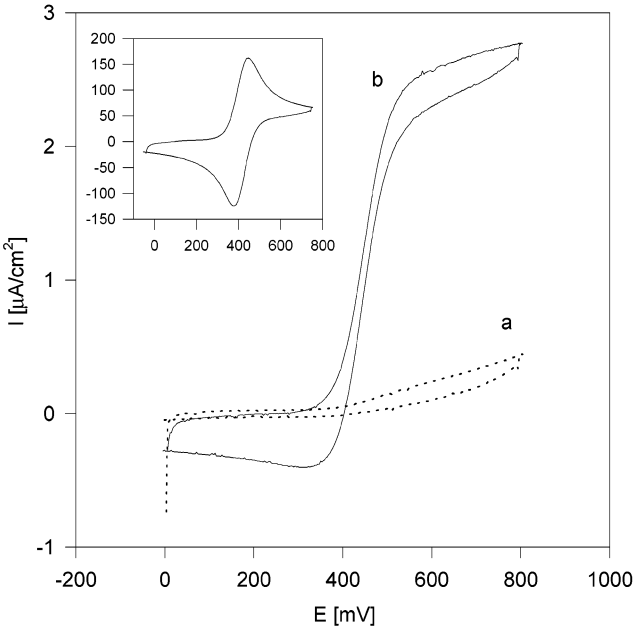

Figure 4. Cyclic voltammograms recorded on gold electrodes covered with (a) C_{18}SH and (b) C_{18}SH/PANI (polymerization charge 14 μC/cm^2) in 1 mM $K_4Fe(CN)_6$ in aqueous 1 M H_2SO_4. Inset: CV curve recorded on bare gold.

A qualitatively different behavior is observed for the thiol/polymer system. Now that the CV curve is sigmoidal in shape, it is not exponential (see the above commentary), and the current values are significantly higher than for nonmodified C_{18}SH. The polarographic-like curves suggest that as a result of polymer deposition the electrode surface is modified in such a way that there exist some areas acting as microelectrodes. The appearance of a heterogeneous surface can stem from two possible reasons: the polymer is deposited on the surface in the form of islands which (being oxidized) act as microelectrodes or, during the electrochemical deposition of the polymer, some new monolayer defects are created and they play the role of microelectrode sites. To answer the question what is the nature of these hypothetical microelectrodes further studies of this system in the presence of a different redox probe, $Ru(NH_3)_6^{3+}$, were performed. The formal potential of this probe is ca. -150 mV, and therefore, in the range of its electroactivity, the polymers are in their reduced nonconducting forms. If the sigmoidal shape of the voltammetric curve in $Fe(CN)_6^{4-}$ solution is the result of the presence of created defects (not plugged with the polymer), a similar layout should be observed in $Ru(NH_3)_6^{3+}$.

On the contrary, when the CV curves of $Ru(NH_3)_6^{3+}$ reduction are exponential, this will mean that the sigmoidal shape of voltammograms in ferrocyanide solution results from the presence of polymer islands on the surface. Figure 5 presents voltammetric curves of $Ru(NH_3)_6^{3+}$ reduction on C_{18}SH and C_{18}SH/PANI-coated gold.

The curve for the unmodified monolayer as expected is characterized by the approximately exponential shape and low magnitude of currents (similarly as for $Fe(CN)_6^{4-}$ a small bend of the curve is observed), whereas the C_{18}SH/PANI layer reveals much smaller currents than unmodified C_{18}SH.

The above results suggest that in consequence of the electrochemical polymerization of monomers the polymer nuclei plug the existing defect sites. However, on the basis of our experiments, we cannot exclude the possibility of the formation of new pinhole defects in the monolayer that are immediately

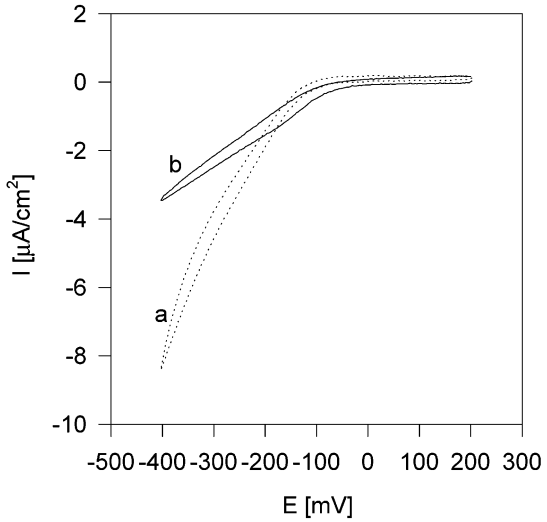

Figure 5. Cyclic voltammograms recorded on gold electrodes covered with (a) $C_{18}SH$ and (b) $C_{18}SH$/PANI (polymerization charge 14 μC/cm^2) in 1 mM $Ru(NH_3)_6Cl_3$ in aqueous 0.5 M KCl.

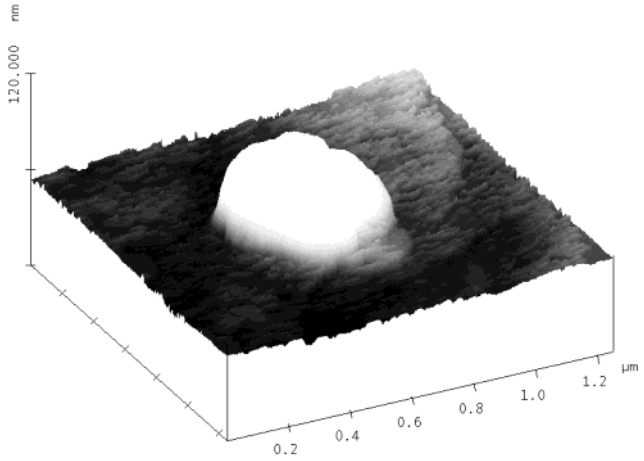

Figure 6. STM image of a typical polyaniline microisland.

filled with the growing polymer. In this scenario, the surface of gold is still insulated from the direct access of hydrophilic redox probes used in our experiments. Depending on the experimental conditions, these polymer nuclei behave like microelectrodes or not.

We obtained qualitatively similar results for two other investigated polymers (poly(o-methoxyaniline) and poly(2,5-dimethoxyaniline)) and various thiol monolayers ($C_{16}SH$ $C_{14}SH$); therefore, they are not presented here.

STM of Polymer Microelectrodes. To confirm the conclusions drawn from electrochemical studies which suggest formation of polymer aggregates on the surface, we used scanning tunneling microscopy to image the polymer structures. Figure 6 presents the STM micrograph of a polyaniline island prepared by electrochemical oxidation of aniline on $C_{18}SH$-coated gold. The island is of approximately cylindrical shape, and it is quite regular. We could find similar polymer features on the surface; however, because of limitations of the size of the scanned area with our STM, we could not reasonably estimate the surface concentration of the structures with this method.

Sometimes in one 10 μm $\times$ 10 μm region of the surface, we were able to locate more than one (e.g., two polymeric islands shown in Figure 7), whereas the neighboring regions were essentially free of nuclei (not shown), suggesting uneven distribution of defect sites. These observations are consistent

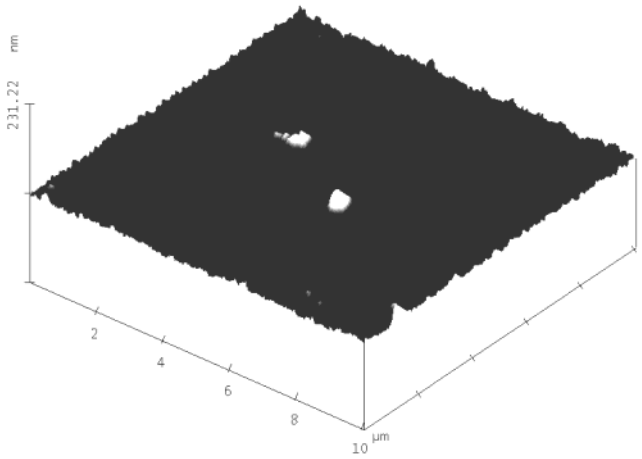

Figure 7. STM image of a polyaniline deposit, an extended scanning area.

with previous reports on similar systems: copper clusters deposited within pinhole sites.[31]

Figure 8 shows a cross section profile of a typical polymer island. It can be read from the graph that the average diameter of the polymer nucleus is ca. 600 nm and its height is ca. 50 nm.

The STM results confirm our previous conclusions on the formation of polymer microelectrodes on the partially blocked surface. Further studies on the distribution of the polymer microstructures were carried out by electrochemical methods.

Growth of the Polymer Islands on the Surface. The investigation of the growth of polymer islands on the surface was based on the observation of evolution of voltammetric curves of $Fe(CN)_6^{4-}$ oxidation as a function of polymerization charge. Figure 9 presents a set of cyclic voltammograms recorded on polyaniline/$C_{18}SH$-coated gold. It can be seen that with the increase of the amount of polymer (measured by the polymerization charge) the oxidation currents of $Fe(CN)_6^{4-}$ increase, and (except for the first curve at $Q = 0$ μC/cm^2) these curves are polarographic in shape. This means that as a result of the monomer oxidation the polymer microelectrodes are created.

The question can be raised however what is the mechanism of the nuclei growth. To answer this question, we analyzed our experimental data from the point of view of the theoretical model provided by Amatore and co-workers.[32]On the basis of the magnitude of limiting current as well as the shift of the half-wave potential with respect to the formal potential of redox couple, we could evaluate the average surface concentration and diameters of the microelectrodes. Figure 10 shows the calculated microelectrode diameters for polyaniline deposited on $C_{18}SH$, $C_{16}SH$, and $C_{14}SH$ as a function of charge consumed for polymerization.

Although the estimation of the microelectrode diameters is obviously very rough, it can be seen that the obtained values are comparable to these obtained from STM measurements. The nuclei diameter is the highest when the polymer is deposited on $C_{18}SH$ and decreases with the decrease of the hydrocarbon chain length of thiols used to form the monolayer. In all these three cases, the diameter increases slightly with the polymerization charge or remains at the same level.

Figure 11 presents the calculated values of the surface concentration of microelectrodes. The number of polymer features increases with the polymerization charge and is in the range of thousands per cm^2. The number of nuclei is the highest for $C_{18}SH$ and decreases for shorter thiols.

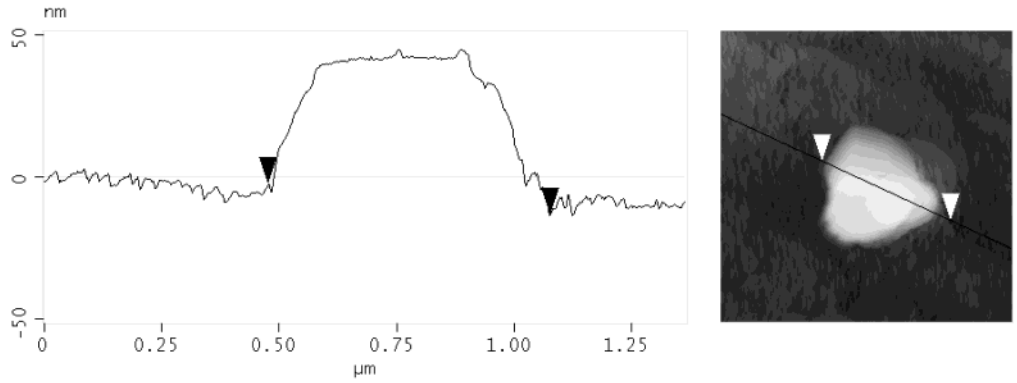

Figure 8. Cross section profile through a polymer microisland.

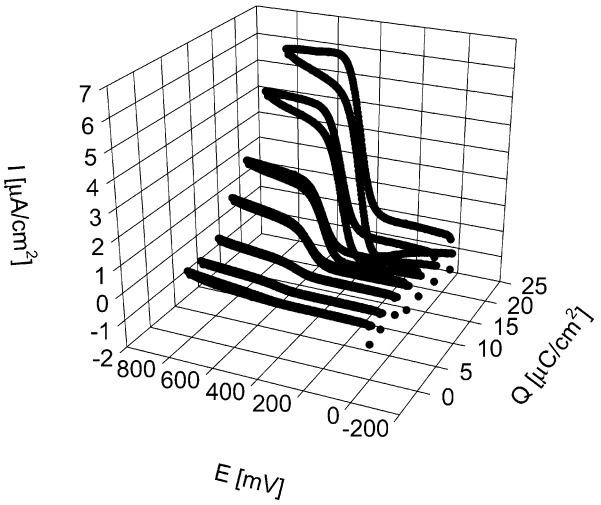

Figure 9. Cyclic voltammograms recorded on gold electrodes covered with $C_{18}SH$/PANI in 1 mM $K_4Fe(CN)_6$ in aqueous 1 M H_2SO_4 for various polymerization charges.

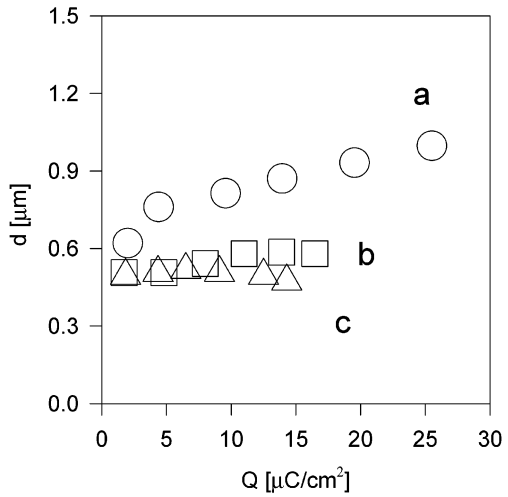

Figure 10. Variation of the average polyaniline microelectrode diameters with polymerization charge. Microstructures prepared on gold covered with (a) $C_{18}SH$, (b) $C_{16}SH$, and (c) $C_{14}SH$.

An interesting question can be asked how the density of polymer microstructures on the surface correlates with the pinhole density of a native monolayer. As it was mentioned above, the CV curves for the case of thiol-coated electrodes both in $Fe(CN)_6^{4-}$ and $Ru(NH_3)_6^{3+}$ reveal only very small bend suggesting the presence of an extremely low amount of small monolayer defects. This creates real difficulties in determination of their exact size and distribution on the basis of the

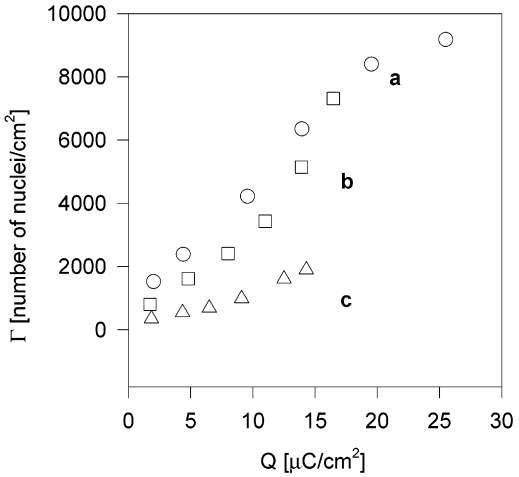

Figure 11. Variation of the polyaniline microelectrode surface concentration with polymerization charge. Microstructures prepared on gold covered with (a) $C_{18}SH$, (b) $C_{16}SH$, and (c) $C_{14}SH$.

electrochemical data. According to a relatively broad literature on the thiol monolayer defects, their size is typically in the range of tens of nanometers, and the distance between them changes from tens to hundreds of micrometers.[31,33,34] The surface concentration of the polymer deposits determined by us is in the range of thousands per cm^2, and it can be easily recalculated to distance between the nuclei.[19] That gives the numbers from ca. 50 to 300 μm. This suggests that the number of polymer deposits is practically comparable to the number of pinhole sites in the monolayer. When the nuclei are initiated in the nanometer-sized defects, then they grow to form islands of micrometer dimensions (which is manifested by relatively large magnitude of $Fe(CN)_6^{4-}$ oxidation current).

Some general conclusions can be drawn on the basis of the above results. In consequence of monomer oxidation on electrodes covered with $C_{18}SH$ $C_{16}SH$ and $C_{14}SH$, polymer islands are deposited starting their growth most probably from defect sites of the monolayers. The dimensions of the nuclei are relatively constant, but their number increases during the deposition process. This means that the growth of a single nucleus is practically instantaneous (in the time scale of the experiment), but the creation of the nuclei (globally) on the surface is progressive (it is not clear if this is the effect of formation of new defects immediately filled with polymer or energetic nonequivalence of native pinholes). Some differences in the amount and dimensions of the polymer microislands are probably the effect of different "crystallinity" of the thiol monolayers. It is well-known that the monolayers consisting of the molecules containing short hydrocarbon chains reveal properties of two-dimensional liquids, but when the length of

the chains increases, their crystallinity is more pronounced.[35] In this case, the movements of the molecules in the two-dimensional space are limited, and the eventual monolayer defects are well-defined. Therefore, when the thiols contain longer chains, the monolayer defects are more stable and they can be more easily modified with polymer deposits. It is understandable therefore that the polymer nuclei are created easily in the $C_{18}SH$ layer as compared to the $C_{16}SH$ and $C_{14}SH$ layers.

It is interesting to note that in the case of molecules containing shorter (that described here) hydrocarbon chains the polymer nuclei are not created at all which is the effect of liquidity of such layers.[36] The defects in these layers are statistical and originate from the dynamics of the liquid in two dimensions.

On the contrary, the well-defined defects in long-chain monolayers make it easier for the nucleation of polymer structures and their immediate growth toward larger sizes.

The growth of the nuclei is probably associated with partial desorption of thiol molecules around the nuclei, but the uncovered metal is immediately coated with the polymer. For shorter more liquid monolayers, both nucleation and growth seems to be more difficult and this results in a smaller number of polymer microelectrodes and their smaller dimensions.

Poly(*o*-methoxyaniline) and Poly(2,5-dimethoxyaniline). The above discussion concerning the formation of polymer microislands using thiol monolayers as templates was illustrated with the data recorded mainly for polyaniline. It should be stressed however that practically identical both qualitative and quantitative (when referred to the same polymerization charge) results were obtained for two other polymers: poly(*o*-methoxyaniline) and poly(2,5-dimethoxyaniline). However, the experimental data for these polymers are not presented here as they do not add anything new to the discussion on the preparation of polymer microelectrodes.

Conclusions

This paper presents the results concerned with synthesis and electrochemical characterization of polymer microelectrodes deposited on gold blocked with thiol monolayers.

Our studies show that the thiol monolayers can be used as molecular matrixes to selectively deposit polymeric material. The defects existing (or purposefully introduced) in the monolayer can be utilized to initiate localized formation of polymer microstructures. The microstructures are created progressively, and their number and distribution depend on the thickness of the thiol monolayers (length of hydrocarbon chains).

The polymer microislands reveal very interesting electrochemical properties. When they are oxidized, they are conducting and behave like an array of microelectrodes. When they are in reduced form because of their nonconductive state, they reversibly lose their microelectrode character. Therefore, the polymer nuclei can be easily switched between conducting and nonconducting forms which may find technological applications, e.g., in chemical analysis or microelectronics.

Acknowledgment. Special thanks are due to Dr. G. Aloisi and Prof. R. Guidelli for the possibility of preparing gold covered glass slides. This work was funded by Grant No. 3 TO9A 117 19 from the Polish Committee for Scientific Research.

References and Notes

(1) Lin S.-Y.; Chow, E.; Hietala, V.; Villeneuve, P. R.; Joannopoulos, J. D. *Science* **1998**, *282*, 274.
(2) Painter, O. *Science* **1999**, *284*, 1819.
(3) Haginoya, C.; Ishibashi, M.; Koike, K. *Appl. Phys. Lett.* **1997**, *71*, 2934.
(4) Gau, H.; Herminghaus, S.; Lenz, P.; Lipowsky, R. *Science* **1999**, *286*, 46.
(5) Velev, O. D.; Kaler, E. W. *Langmuir* **1999**, *15*, 3693.
(6) Skotheim, T. A.; Elsenbaumer, R. L.; Reynolds, J. R. *Handbook of Conducting Polymers*, 2nd ed.; Marcel Dekker: New York, 1998.
(7) MacDiarmid, A. G.; Mu, S.-L.; Somasiri, N. L. D.; Wu, W. *Mol. Cryst. Liq. Cryst.* **1985**, *121*, 187.
(8) Kobayashi, T.; Yoneyama, H.; Tamura, H. *J. Electroanal. Chem.* **1984**, *161*, 419.
(9) Inzelt, G.; Pineri, M.; Schultze, J. W.; Vorotyntsev, M. A. *Electrochim. Acta* **2000**, *45*, 2403.
(10) Willicut, R. J.; McCarley, R. L. *J. Am. Chem. Soc.* **1984**, *116*, 10823.
(11) Krysinski, P.; Jackowska, K.; Mazur, M.; Tagowska, M. *Electrochim. Acta* **2000**, *46*, 231.
(12) Major, J. S.; Blanchard, G. J. *Langmuir* **2001**, *17*, 1163.
(13) Kohli, P.; Blanchard, G. J. *Langmuir* **1999**, *15*, 1418.
(14) Kohli, P.; Blanchard, G. J. *Langmuir* **2000**, *16*, 4655.
(15) Kohli, P.; Blanchard, G. J. *Langmuir* **2000**, *16*, 8518.
(16) Mazur, M.; Krysinski, P. *Langmuir* **2001**, *17*, 7093.
(17) Parthasarathy, R.; Martin, C. R. *Nature* **1994**, *369*, 298.
(18) Mazur, M.; Krysinski, P. *Langmuir* **2000**, *16*, 7962.
(19) Mazur, M.; Krysinski, P.; Jackowska, K. *Thin Solid Films* **1998**, *330*, 167.
(20) Krysinski, P.; Brzostowska-Smolska, M.; Mazur, M. *Mater. Sci. Eng. C* **1999**, *8*−*9*, 551.
(21) Schessler, H. M.; Karpovich, D. S.; Blanchard, G. J. *J. Am. Chem. Soc.* **1996**, *118*, 9645.
(22) Kohli, P.; Taylor, K. K.; Harris, J. J.; Blanchard, G. J. *J. Am. Chem. Soc.* **1998**, *120*, 11962.
(23) Karpovich, D. S.; Blanchard, G. J. *Langmuir* **1997**, *13*, 4031.
(24) Krysinski, P.; Brzostowska-Smolska, M. *J. Electroanal. Chem.* **1997**, *424*, 61.
(25) Li, X.; Zhang, X.; Sun, Q.; Lu, W.; Li, H. *J. Electroanal. Chem.* **2000**, *429*, 23.
(26) Hayes, W. A.; Kim, H.; Yue, X.; Perry, S. S.; Shannon, C. *Langmuir* **1997**, *13*, 2511.
(27) Hayes, W. A.; Shannon, C. *Langmuir* **1998**, *14*, 1099.
(28) Heckl, W. M. In *Procedures in Scanning Probe Microscopies*; Colton, R. J., Engel, A., Frommer, J. E., Gaub, H. E., Gewirth, A. A., Guckenberger, R., Rabe, J., Heckl, W. M., Parkinson, B., Eds.; John Wiley and Sons: New York, 1998; p 76.
(29) Marcus, R. A.; Sutin, N. *Biochim. Biophys. Acta* **1985**, *811*, 265.
(30) Yang, R.; Qian, Z.; Deng, J. *J. Electrochem. Soc.* **1998**, *145*, 2231.
(31) Finklea, H. In *Electroanalytical Chemistry*; Bard, A. J., Rubinstein, I., Eds.; Marcel Dekker: New York, 1996; Vol.19, p 110.
(32) Amatore, C.; Saveant, J. M.; Tessier, D. *J. Electroanal. Chem.* **1983**, *147*, 39.
(33) Diao, P.; Guo, M.; Tong, R. *J. Electroanal. Chem*. **2001**, *495*, 98.
(34) Bilewicz, R.; Majda, M. *J. Am. Chem. Soc.* **1991**, *113*, 5464.
(35) Krysinski, P.; Moncelli, M. R.; Tadini-Buoninsegni, F. *Electrochim. Acta* **2000**, *45*, 1885.
(36) Mazur, M.; Krysinski, P.; Palys, B. *J. Electroanal. Chem.* Accepted for publication.